Determination of the Optimal Coverage for Heavy-Duty-Axle Gears in Shot Peening

Hongzhi Yan
State Key Laboratory of High Performance Complex Manufacturing, College of Mechanical and Electrical Engineering, Central South University, Changsha, 410083, PR China

Pengfei Zhu
State Key Laboratory of High Performance Complex Manufacturing, College of Mechanical and Electrical Engineering, Central South University, Changsha, 410083, PR China

Zhi Chen (zhichen415@gmail.com)
State Key Laboratory of High Performance Complex Manufacturing, College of Mechanical and Electrical Engineering, Central South University

Hui Zhang
State Key Laboratory of High Performance Complex Manufacturing, College of Mechanical and Electrical Engineering, Central South University, Changsha, 410083, PR China

Yin Zhang
State Key Laboratory of High Performance Complex Manufacturing, College of Mechanical and Electrical Engineering, Central South University, Changsha, 410083, PR China

Yu Zhang
Central South University of Forestry and Technology, Changsha, 410004, PR China

Research Article

Keywords: Shot peening, Heavy-duty-axle gear, The optimal coverage, Surface integrity

Posted Date: April 30th, 2021

DOI: https://doi.org/10.21203/rs.3.rs-453575/v1

Version of Record: A version of this preprint was published at The International Journal of Advanced Manufacturing Technology on September 5th, 2021. See the published version at https://doi.org/10.1007/s00170-021-07964-w.

Determination of the optimal coverage for heavy-duty-axle gears in shot peening

Hongzhi Yan[1], Pengfei Zhu[1,2], Zhi Chen[1], Hui Zhang[1], Yin Zhang[1], Yu Zhang[3]

Abstract

Pitting and wear often appear on heavy-duty-axle gears due to their harsh working conditions, such as high torques, high loads and poor lubrication. Shot peening is a popular surface strengthening method for gears. In order to ensure complete coverage during shot peening, 100%~200% coverage is usually prescribed for most gears. However, it is difficult to effectively improve the contact fatigue and wear resistance of heavy-duty-axle gears. Generally, increasing shot peening coverage can heighten the compressive residual stress for prolonging the service lifetime of gears. Whereas, high coverage levels may cause the deterioration of surface roughness, thus increase the noise and vibration of gears. To address this issue, this paper deals with the determination of optimal coverage for heavy-duty-axle gears by experimental tests. The influence of shot peening coverage on the surface integrity of gears is analyzed in terms of residual stress, microhardness, surface morphology and dislocation density. The results show that the maximum compressive residual stress increases first and then keeps stable with the increase of coverage, and the maximum value is −1172.10 MPa. The microhardness peak increases obviously in the beginning and then slowly rises with the increase of coverage, and the maximum value is 747.5 $HV_{1.0}$. The surface roughness (*Ra*) decreases initially and then enhances with the increase of coverage, and the minimum value is 0.99 μm under the coverage of 1000%. The dislocation density increases with the increase of coverage, and the maximum value is 3.70×10^{16} m^{-2}. Numerous damages (microscalings, spallings) occur on the treated gear tooth flank affecting the residual stress distribution and roughness under high coverage levels. Taking into consideration of service lifetime, working noise and economic efficiency, the coverage of 1000% is the optimal coverage for heavy-duty-axle gears in shot peening.

Keywords Shot peening · Heavy-duty-axle gear · The optimal coverage · Surface integrity

1 Introduction

Spiral bevel gears mounted on the drive axle are key transmission parts for heavy-duty vehicles. The meshing gear pair suffers from percussive load, high torque and harsh running conditions, thus initial pitting and wear failures often occur on the gear tooth flanks [1,2]. Shot peening is a cold working process, wherein a lot of shots with high hardness and high speed strike the surface of the workpiece and induce compressive residual stress for the improvement of the anti-fatigue performance of the workpiece [3]. It is a common gear surface strengthening method, and is usually combined with heat treatment processes in the process of gear manufacturing like carburization, nitridation, nitrocementation, etc. Typically, the load-carrying capacity of a gear can be increased by 20% to 30 % after shot peening [4]. More importantly, without increasing the size and weight of the gear or changing novel materials, designers can improve the fatigue strength of the gear through shot peening, so it can reduce manufacturing cost and improve fuel efficiency from the aspect of economy and ecology [5]. In addition, shot peening can induce tiny indentations on the tooth flank as very small oil reservoirs which help to promote lubrication, reduce wear, spalling, scoring and lower operating temperature by reducing friction [6-9]. Shot peening can eliminate the tool marks left by machining and reduce the stress concentration on gear tooth flanks [10]. Surface abnormal layer can be reduced by shot peening [11]. Therefore, shot peening is such a process that can improve the fatigue

✉ Zhi Chen

zhichen415@gmail.com Tel.+8618202764498

1 State Key Laboratory of High Performance Complex Manufacturing, College of Mechanical and Electrical Engineering, Central South University, Changsha, 410083, PR China

2 Kaifeng University, Kaifeng, 475004, PR China

3 Central South University of Forestry and Technology, Changsha, 410004, PR China

strength, load-carry capacity of gears and can meet the requirements of lightweight design of gears.

Coverage is one of the most important parameters in the shot peening process, and other parameters such as shot peening intensity, shot peening pressure, mass flow rate, shot size, impact angle and distance from nozzle to workpiece are all related to it. Coverage is defined as the percentage of a given surface area actually impacted by shot peening (dimpled surface) [12]. It is proportional to shot peening time [13]. Coverage beyond 100% (i.e., 200%, 300%) is defined as multiples of the time taken to achieve 100% coverage (i.e., 2×, 3×) [14]. There are some methods to verify the coverage of peened gears [14,15], including fluorescent tracer dyes, optical analyzers, dye marker inks, etc. Considering production cost, processing efficiency and shot wear, manufacturers usually select 100% or 200% coverage to ensure the uniform injection of gears. However, they rarely pay attention to higher coverage levels of gears. For the maximum improvement of fatigue and wear resistance of gears, 100%~200% coverage may not be the optimum value. Different materials and shapes of parts have their most appropriate coverage, so reasonable selection and control coverage levels can achieve the best shot peening effect [16].

Most of the changes of surface integrity of workpieces induced by shot peening may affect the success of the treatment. Shot peening coverage has great effects on the surface integrity of workpieces. Wu et al. [17] investigated the effect of shot peening with 100% and 200% coverage on the hardness, residual stress and grain size for 18CrNiMo7-6 carburized gear steel. Maleki et al. [18] studied the effect of shot peening coverage on properties of AISI 1045 carbon steel, of which the shot intensity was 27A, and the coverage were 100%, 500%, 1000% and 1500%, respectively. The results indicated that compressive residual stress distribution was increased slightly with coverage, whereas the amount of grain refinement was directly related to coverage. Microhardness of the peened workpiece in high coverage was significantly increased, and the surface roughness enhances with the increase of coverage until reached a stable value. Whereafter, Maleki et al. [19] detected the influence of coverage on hardness, grain size and residual stress of AISI 1060 steel by orthogonal test. The results indicated that the weight values of coverage affecting microhardness, grain size and residual stress were 68%, 89% and 57%, respectively. Inoue et al. [20] found that for SCM415 spur gears, the surface hardness of tooth root could increase 30-80 HV with the increase of shot peening coverage (150%~600%) and intensity (0.25~0.85 mmA), and the coverage has little influence on the residual compressive stress near the gear root. However, the coverage variation range is not wide in Inoue's study. Santa-aho et al. [10] studied the effect of shot peening on the tooth surface roughness of 17NiCrMo6-4 carburized gear through scanning electron microscope (SEM) characterization experiment. The results showed that increasing the shot-peening intensity and coverage density at the same time could reduce the surface roughness when gears were harder than the shots used in the experiment. Based on the review of many researchers' studies, the studies are mainly focused on gear steels and spur gear roots. The failure mechanism for tooth flanks and tooth roots is different, and the key surface integrity parameters differ from tooth roots and flanks. Thus, it is indispensable to investigate the surface integrity of gear flanks under different coverage. More importantly, the machining methods for spiral bevel gears (i.e., face hobbing or face milling) resulting in different surface integrity after peening. Furthermore, the study on surface integrity of gears or gear steels treated by shot peening is incomprehensive, such as the evolutionary mechanism of microstructure. In particular, the quantitative analysis of the microstrain and dislocation density on the gear tooth flank after shot peening is rarely reported. And then, the understanding of effects of coverage on residual stress distributions is still not clear, and sometimes it exists some debatable results as shown in Refs. [17,18,20-22]. Finally, investigation scope of shot peening coverage on surface integrity of gears is not wide, and especially high coverage levels which may cause different kinds of surface defects should be considered.

When the heavy-duty vehicle is running on the

road, the drive face of the pinion is prone to pitting because of the high contact stress. So particular attention is paid to the drive face of a pinion in this paper. Aiming to determine of the optimal coverage for heavy-duty-axle gears in shot peening, the effect of shot peening coverage on surface integrity of gear tooth flanks is investigated by experimental characterization. A wide range of coverage levels (100%, 500%, 1000%, 2000%, 4000%) are selected in this research. The investigated surface integrity parameters include residual stress distribution, microhardness, surface roughness, microtopography, dislocation density, etc. The research has high engineering value for shot-peening parameters selection to improve contact fatigue and wear resistance of gears.

2 Experiment setup

2.1 Material and specimens

The subject of the research is spiral bevel gears for the heavy-duty axle, and 5 specimens are processed in the same batch made of 22CrMoH gear steels. The measured chemical composition of the steel is tabulated in Table 1. The gear module and tooth number for each specimen are 10.345 mm and 24, respectively. As shown in Fig. 1, the processing of the test gears is mainly divided into the following stages: forging, normalizing, face hobbing, heat treatment, shot peening. Thereinto, heat treatment process consists of carburizing, quenching, and low temperature tempering. Then the gears have the effective case depth (depth to 550 HV) of about 1.7 mm, the surface hardness and core hardness are about 59~64 HRC and 33~45 HRC, respectively.

Table 1 Chemical composition of 22CrMoH alloys

Elements	C	Mn	P	S
Content(wt. /%)	0.203	0.861	0.009	0.0283
Elements	Si	Cr	Mo	Fe
Content(wt. /%)	0.259	1.16	0.411	balance

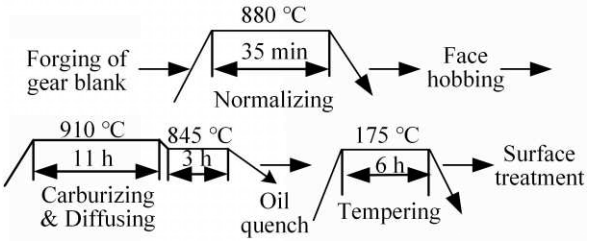

Fig. 1 Machining and heat-treatment process

2.2 Shot peening treatment

Shot peening experiment is performed with an automatic compressed air shot peening equipment (Liangshi, LSSKPWJP-8). The gear specimen for each test is fixed on the worktable and rotates with its own central axis under the jet stream. The nozzle moves along the root cone of the gear. Each station of the machine is equipped with 4 nozzles, and 4 nozzles with a slight offset process a gear simultaneously. The inner diameter of the nozzle is 8 mm, the moving speed of the nozzle is 3 mm/s, the distance from nozzle to work-piece is controlled as 150 mm. For the complex gear shapes, the impact angle and worktable rotational speed are set as 50° and 25 r/min, respectively. The shot peening pressure is 0.45 MPa, and mass flow rate is set to be 13 kg/min. Thus, the shot velocity is controlled by adjusting shot peening pressure and feed valve setting. The shot peening process is shown in Fig. 2. Cut wire shots (CCW-32/G3) with a diameter of 0.8 mm are used in this work, and the average hardness of the measured shots is 61.1 HRC.

A-type Almen strip is used to measure the shot peening intensity, which is 0.66 mmA according to SAE J443 standard [23]. The method of dye marker inks is used to verify the coverage according to SAE J2277 [15]. It is found that the nozzle moving along the root cone of the gear for one time can guarantee a coverage of 100%, thus the coverage of 500%, 1000%, 2000%, 4000% are shot peening for 5 times, 10 times, 20 times, and 40 times, respectively. The 5 specimens in this work are marked as SP1 (100% coverage), SP5 (500% coverage), SP10 (1000% coverage), SP20 (2000% coverage), and SP40 (4000% coverage), respectively. Several gear teeth are cut off by wire cut electrical discharge machining (DEDM) from each specimen for subsequent characterization

tests.

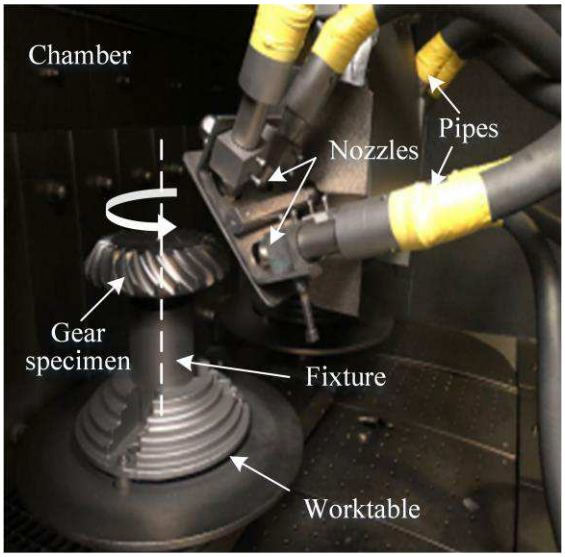

Fig. 2 Shot peening of the gear

2.3 Testing methods

2.3.1 Mechanical property measurements

Mechanical property measurements include residual stress and microhardness test. According to the standards of ASTM-E915-2010 [24] and EN 15305-2008 [25], the residual stress measurement is carried out by Proto-iXRD X-ray stress analyzer with V filter. The measurement is performed by means of Omega mode (ISO inclination). The measurement location is at the flank center in the profile direction. The measurement is made using Cr-Kα radiation and the {211}-Fe reflection crystallographic plane. The irradiated area size is 1 mm in diameter. The tube voltage and current are set to be 25 kV, 5 mA, respectively. In order to get the in-depth residual stress distributions, an electropolisher (Proto, 8818-V3) is used to remove surface materials stepwise in the detection site with saturated sodium chloride solution. The Moore and Evans procedure is used to correct the results of the in-depth residual stress measurements related to material removal [26]. The voltage and current set in the electrolytic polishing machine are 60 V and 2 A, respectively. A VHX-5000 3D microscope with super wide depth of field is used to measure the removed depth of the surface material each time.

Hardness distribution along the depth is measured with Huayin 200HVS-5 digital Vickers hardness tester with experimental force of 9.807 N and loading time of 10 s. The microhardness is measured on the cross-section of gears from the treated surface (near the pitch circle) to the core of the gear with a spacing of 0.1 mm. Before measuring abrasive papers are used to grind the cross section of the gear teeth to ensure that the surface state cannot affect the hardness results. In order to avoid measurement errors, 3 measurements are made at each depth, and the average value is taken as the final result.

2.3.2 Surface morphology measurements

Surface morphology measurements include surface roughness test and microtopography observation. Before the observation of surface morphology, gears are cleaned in alcohol solution by ultrasonic cleaners. Optical profilometer (Wyko, NT9100) equipped with the Vision software is used to measure the surface roughness values and surface roughness profile at the central area of the gear tooth flank for each specimen. The measured area is about 1 mm^2, and 5 times of the eyepiece is used. After 3 measurements of the most representative roughness parameters, including the arithmetic average roughness value (Ra), the total height of the profile height (Rt), root mean squared surface roughness (Rq) and the maximum height of the profile (Rz), the average value is taken as the final result for each surface roughness parameter.

For further analysis, a field emission scanning electron microscope system (TESCAN, MIRA 3 LMU) is used to characterize the micromorphology of the treated tooth flank for each specimen. Especially, it aims at determining the damages on the tooth flank with the increase of shot peening coverage.

2.3.3 X-ray diffraction measurements and calculations

X-ray diffraction (XRD) diffractometer (Brock, Advance D8) is used to qualitatively analyze XRD patterns of the tooth flank treated with different shot peening coverage. The instrument is operated with

Cu-Kα radiation (voltage 40 kV, current 40 mmA); the scanning speed, step and scanning angle are set to be 2°/min, 0.02°, and 40°~129°, respectively.

Based on the XRD, Williamson-Hall (W-H) method is used to study the evolution of microstrain and dislocation density on the tooth flank [27-29]. The W-H equation could be expressed as:

$$\delta\frac{\cos\theta}{\lambda}=\frac{k}{D}+2\varepsilon\frac{\sin\theta}{\lambda} \quad (1)$$

Here, D, λ, θ, ρ and ε are domain size, X-ray wave-length (0.15418 nm), diffraction angle, dislocation density, and microstrain, respectively. k is the Scherer's factor, which is 0.9. δ is the normalized XRD peak width obtained by Gaussian relations, which is give as:

$$\delta=\sqrt{\delta_{\mathrm{m}}^{2}-\delta_{0}^{2}} \quad (2)$$

Where δm is experimentally measured XRD peak width and δ_0 is the instrumental correction of peak width obtained by silicon-640 standard specimen. In fact, δ, δm and δ_0 here represent full widths at half maximum (FWHM).

Williamson and Smallman [28] pointed out that only considering the lattice distortion caused by the variation of dislocation density in the material, the dislocation density ρ and the microstrain ε could be expressed as:

$$\rho=14.4\frac{\varepsilon^{2}}{b^{2}} \quad (3)$$

Here, b is the value of the Burgers vector (0.248 nm for steel) [30].

3. Results and discussions

3.1 Mechanical property

3.1.1 Residual stress

The influence of shot peening coverage on residual stress distribution on tooth flank is shown in Fig. 3. Because of plastic deformation and Hertz contact pressure [31], shot peening increases the magnitude of compressive residual stress on the external surface of the gear, and maximum compressive residual stress locates on the subsurface. Subsequently, with the increase of layer depth, the magnitude of compressive residual stress then decreases and gradually tends to be stable. It is concluded that increasing coverage level may not always result in a high magnitude of compressive residual stress on the external tooth surface. Similar results were reported by Refs. [10,32]. As shown in Fig. 3, the residual stress on the external surface of all peened specimens ranges from −518.53 to −634.71 MPa, and the value of SP1 is the highest. The reason may lie in surface damages caused by high shot peening coverage levels [33]. These results may suggest that if we intend to obtain a high compressive residual stress distribution on tooth flanks by increasing shot peening coverage, it should be considered the surface state of gears.

The measured maximum compressive residual stress is located at the depth of 50~75 μm, and fluctuates from −852.63 to −1172.10 MPa. The maximum compressive residual stress is helpful to restrain the crack propagation and improve the fatigue resistance of the gear. The maximum compressive residual stress for coverage levels less than 1000% exhibits obvious growth tendency with coverage. Beyond the coverage of 1000%, there are no significant variations in the magnitude of maximum compressive residual stress, indicating that compressive residual stress has a saturation value [34]. AGMA [14] reported the maximum residual compressive stress was about 50%-60% of the ultimate tensile strength (UTS) of the peened gear surface. Accordingly, the maximum compressive residual stress of the gear produced by shot peening cannot increase indefinitely.

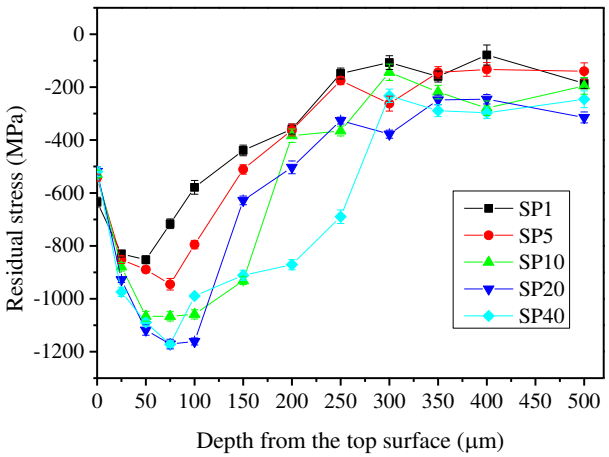

Fig. 3 Residual stress depth profiles in the gear

profile direction. SP1 (100%), SP5 (500%), SP10 (1000%), SP20 (2000%), SP40 (4000%).

3.1.2 Microhardness

In general, the microhardness value of the material after shot peening is used to characterize the cold hardening characteristics of the material. Fig. 4 exhibits the microhardness variation versus coverage. Each data point represents the mean value of 3 different indentations at the same depth, and the error bars represent the mean standard deviations. It can be concluded that the variation trend of the surface microhardness of the peened gear is basically the same. Due to Hertz pressure, the hardness peak occurs in the near-surface layer, and the microhardness decreases gradually with layer depth. This is due to the reduction of grain refinement, martensite phase transition, dislocation density, and plastic deformation induced by shot peening along the in-depth direction. The higher hardness gives rise to better contact fatigue and wear resistance of the gear. If hardness gradient changes too quickly, it will tend to form stress concentration points on the gear [35]. It is observed that the decline value of hardness in the depth of adjacent layers does not exceed 30 $HV_{1.0}$. It is revealed that this smooth hardness transition can exert a beneficial effect on contact fatigue and wear behavior. As shown in Fig.4, with the increase of coverage, microhardness values at the depth of 0.1 mm in the near-surface layer increase accordingly, ranging from 656.5~747.5 $HV_{1.0}$. With the increase of coverage, how much increase in hardness peak? From Fig. 4, microhardness of SP40 at the depth of 0.1 mm increased by 13.9% compared with that of SP1. It is indicated that shot peening can promote tooth surface cold work hardening effect with the increase of coverage. However, from SP1 to SP40, the hardness at the depth of 0.1 mm increased by 6.49%, 3.39%, 0.83%, and 2.57%, respectively. It is noted that the increasing trend of the hardness peak slows down. Especially beyond the coverage of 1000%, no obvious changes occur with increasing coverage. This phenomenon indicates that the plastic deformation of the material has reached its limit, and the high dislocation density and carbon content prevent the further accumulation of local plastic strain near the surface [36]. Therefore, it can also be concluded that there exists a saturation value of hardness for shot peened gears under different coverage.

From the microscopic point of view, the improvement of surface microhardness of the gear is due to the evolution of surface microstructure induced by shot peening, that is, the decrease of residual austenite caused by austenite grain refinement and martensite transformation. According to the classical Hall-Petch relationship, the increase of hardness may be attributed to refinement of grains in the surface layer [37]. The martensitic phase transition reflects the level of cold hardening, and is proportional to the residual stress to some extent. The greater residual compressive stress on the surface layer of the material indicates more residual austenite transformation, thus leading to a high microhardness. Therefore, it can be seen that the hardness peak is consistent with the peak value of compressive residual stress shown in Fig 3.

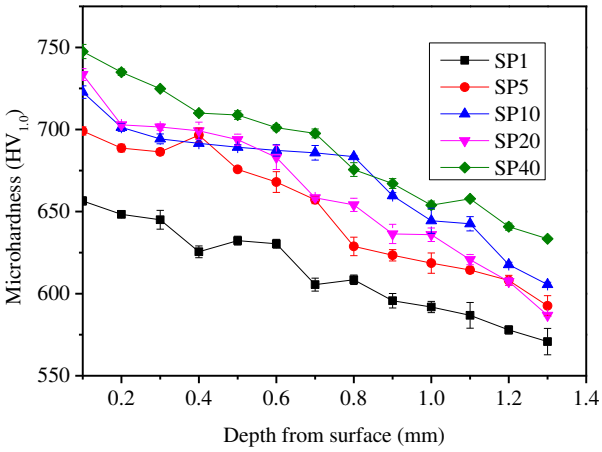

Fig. 4 Microhardness distributions. SP1 (100%), SP5 (500%), SP10 (1000%), SP20 (2000%), SP40 (4000%).

3.2 Surface morphology

3.2.1 Surface roughness

In the automotive field, surface roughness is often considered as the key factor affecting lubrication, contact fatigue resistance and transmission efficiency of gears. Shot peening changes the surface roughness of gears, which is considered as a negative factor.

AGMA [14] pointed out that excessive roughness on active gear tooth flanks produced by shot peening could increase the risk of micro-pitting. The surface roughness of peened gear tooth flanks depends on the machining method, the surface roughness before shot peening, shot peening parameters and so on.

Fig. 5 shows the average surface roughness values in the forms of *Ra*, *Rq*, *Rt*, and *Rz* under different coverage. All surface roughness values are defined according to ISO 25178-2 [38]. What can be observed is that the variation trend of each surface roughness parameter is similar. It is worth noting that the surface roughness decreases with increasing coverage levels, and then increase slightly. Surface roughness reaches the minimum value under the coverage of 1000% in this work. As the first stage of balls impact the surface of the gear, it induces a lot of deep dimples. Due to enhanced cold work hardening of the gear, the successive impacts can only induce shallower dimples, thus playing the role of flattening the earlier peaks. The reason why surface roughness increases under high coverage can be explained by the surface topography of the peened surface. In most of the cases, engineers mainly focus on the surface roughness of *Ra*. From Fig. 5, the surface roughness *Ra* of SP5 is about 21.28% less than that of SP1, whereas the reduction is about 7.15% for *Rz*. It is revealed that proper increase of coverage can reduce the surface roughness of gear tooth flanks, and the results are compatible with that of other literature [10,17,34,39].

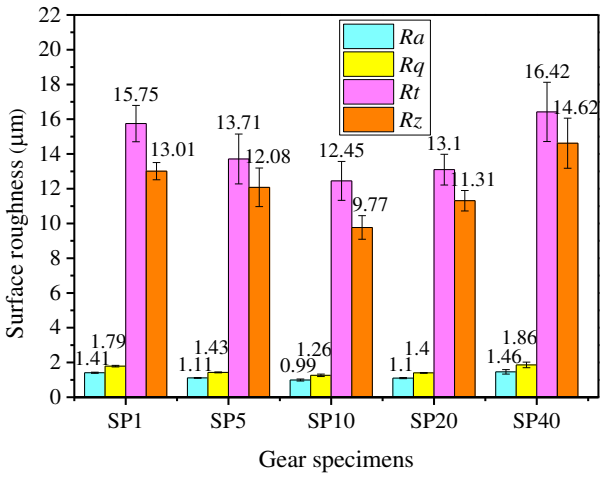

Fig. 5 Surface roughness evolution. SP1 (100%), SP5 (500%), SP10 (1000%), SP20 (2000%), SP40 (4000%).

3.2.2 Microtopography

Fig. 6 presents the surface roughness profiles and SEM observations taken from the peened gear tooth flanks. Fig. 6(a) shows some hobbing marks like knife scars are clearly visible on the surface of SP1, and the texture has directionality. With the increase of coverage, the hobbing marks gradually disappear, surface directionality is diminished, and the plastic deformation introduced by shot peening is increased (Fig. 6(b-e)). The impacts of shots and some surface cavities can be seen on all treated specimens. Fig. 6(a-c) shows very few microscalings on the peened gear surface [10,40]. More notably, Beyond the coverage of 1000%, the population of tooth surface microscalings goes up, the surface layers begin to peel off, and the pallings occur on the peened gear surface as shown in Fig. 6(d). As depicted in Fig. 6(e), the surface is severely damaged and considerable microscalings, spallings and burrs are formed. Such damages created by overlapping of peening dimples and surface plastic deformation can often be found around the hobbing marks or between dimple boundaries, which could cause premature crack initiation on tooth flanks. Some researchers also got the similar SEM characterization observations on other materials [10,41-47]. To conclude, it is inevitable that defects generate on the peened surface of gears as clearly seen in the SEM images. Different shot peening parameters may result in different damages on the surface, so shot peening parameters should be adapted to the gear material and geometry.

The surface microtopographies have good consistency with the surface roughness data presented in Fig. 5. The higher roughness value of the specimen peened with 100% lies in the deep craters induced by shot peening and hobbing marks, which increase the height of peak on the surface. When the coverage reaches to 500% and 1000%, the craters are flattened and hobbing marks are undermined by continuous shot peening bombardment, thereby inducing a smoother surface. Compared with SP5, the smaller roughness value of SP10 is related to the shallower craters and hobbing marks on the surface. The reason why the surface roughness value is larger under excessive coverage (SP20 and SP40) is that

numerous damages and considerable plastic deformation appear on the surface. It is suggested that shot peening above the coverage of 1000% is not recommended because of over-peening.

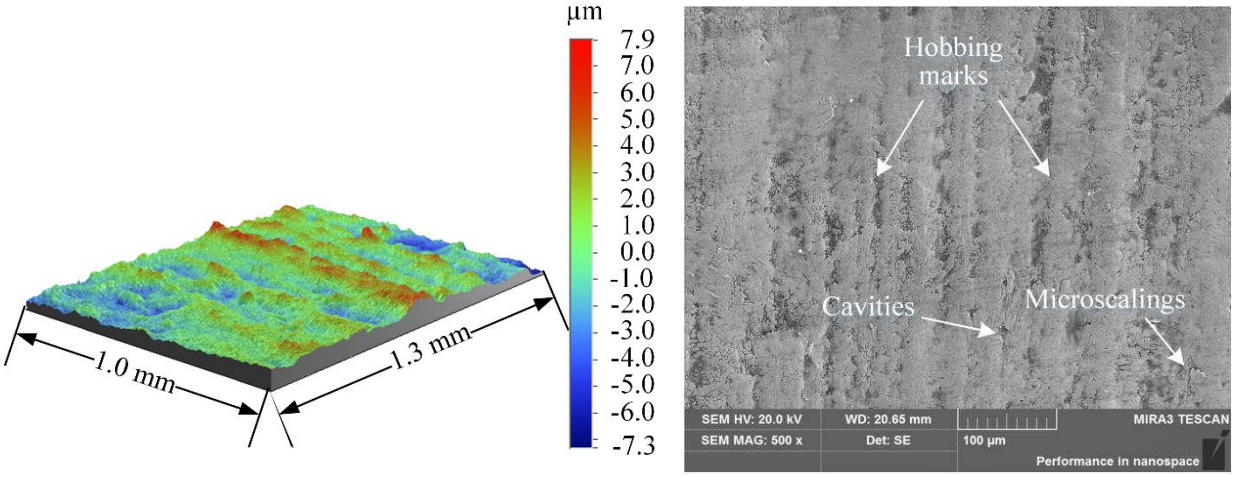

(a) SP1 (100%)

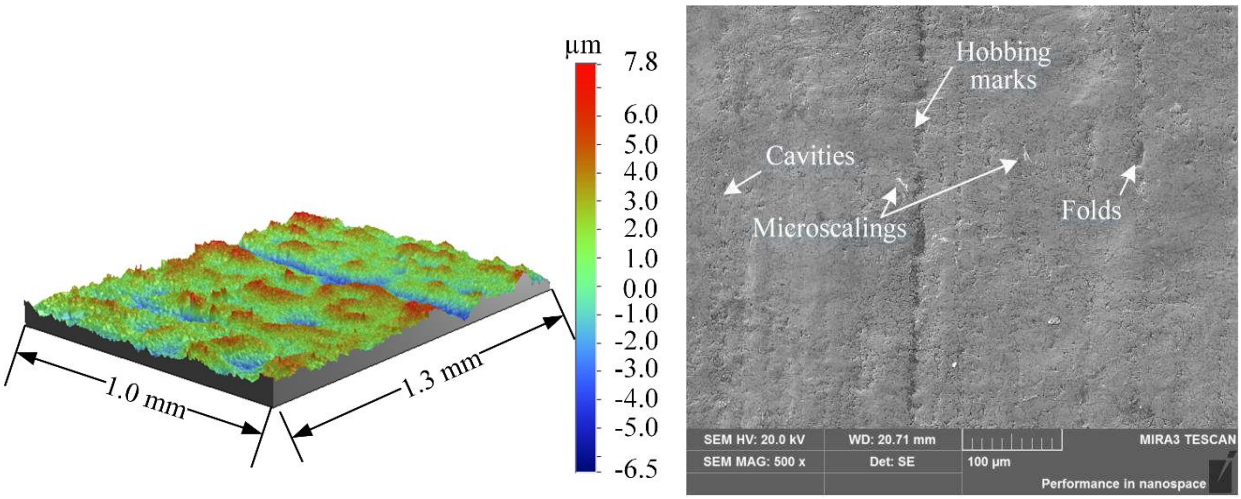

(b) SP5 (500%)

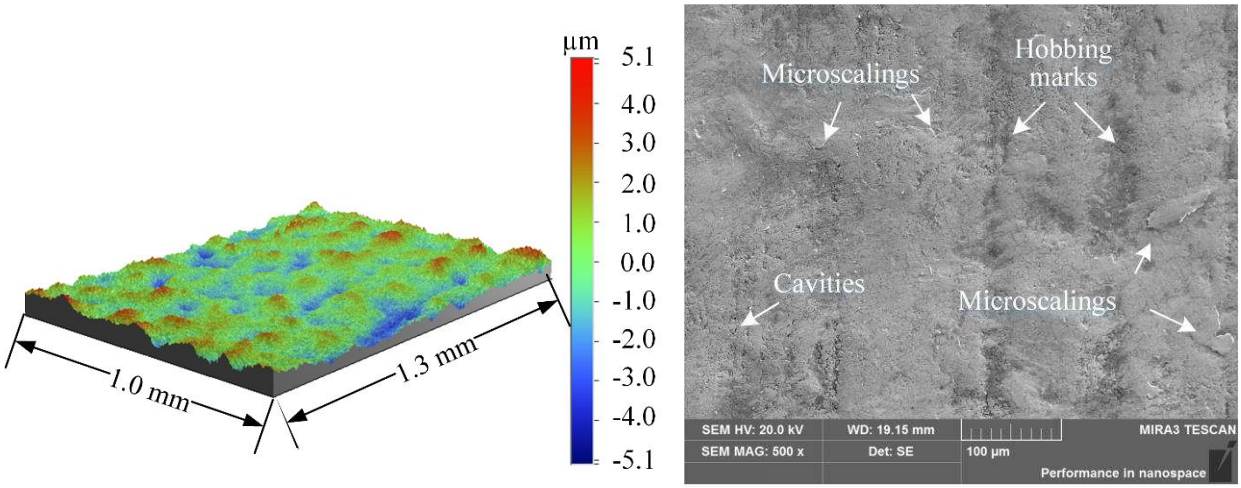

(c) SP10 (1000%)

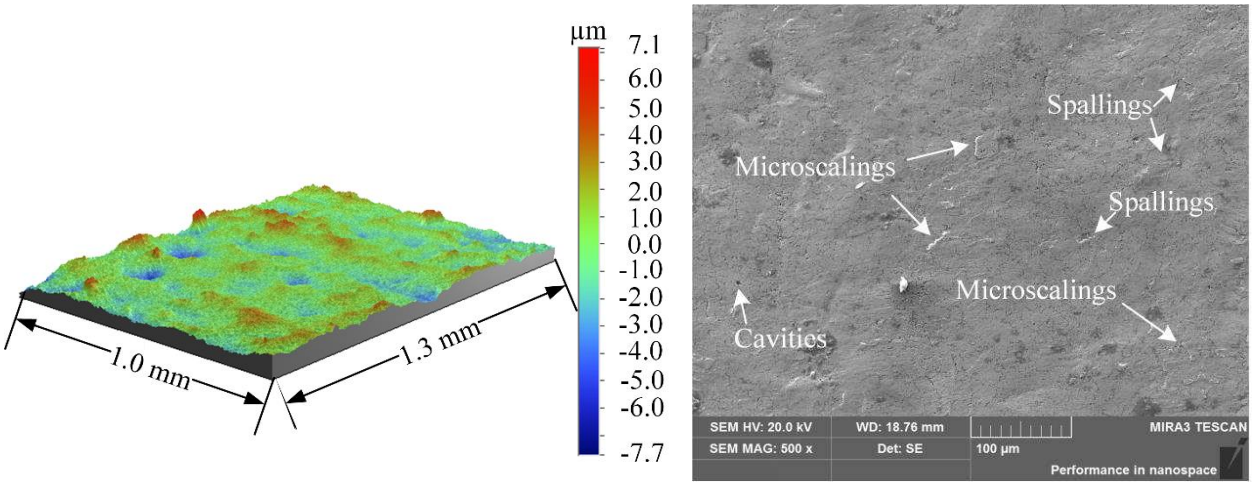

(d) SP20 (2000%)

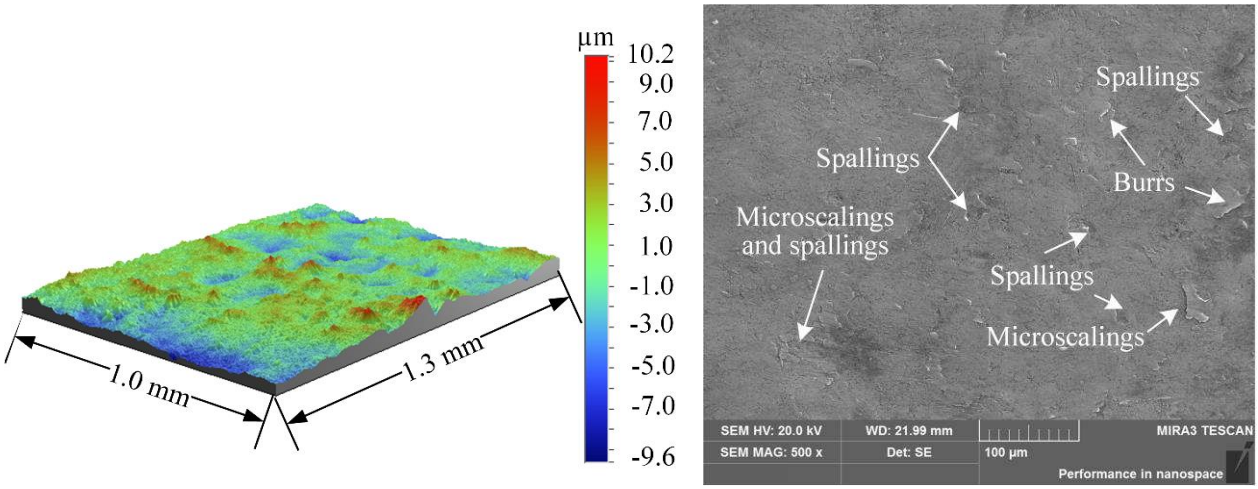

(e) SP40 (4000%)

Fig. 6 Surface roughness profiles (left) and SEM images (right)

3.3 XRD analysis

3.3.1 Phase analysis

Fig. 7 shows the XRD patterns of the topmost surface of the specimens peened with different coverage levels. The number of diffraction peaks does not change, which indicates that the gear treated with different shot peening coverage will not generate new phase [43]. The phase is dominated by martensite (M), which is caused by the transformation from austenite to martensite induced by strain after shot peening. The results are consistent with the findings expressed by other Refs. [48-51]. As depicted in Fig. 7, the FWHM values at the topmost surface for (110) lattice plane increase with coverage levels, and the value of SP40 increases by 32.16% compared with that of SP1. The grain size is negatively correlated with FWHM [52]. Hence, it is revealed that with the increase of coverage, grain size at the topmost surface decreases, whereas FWHM becomes wider. This is due to plastic deformation occurs on the gear surface layer induced by continuous impacts of shot streams, which leads to grain refinement and lattice distortion [53].

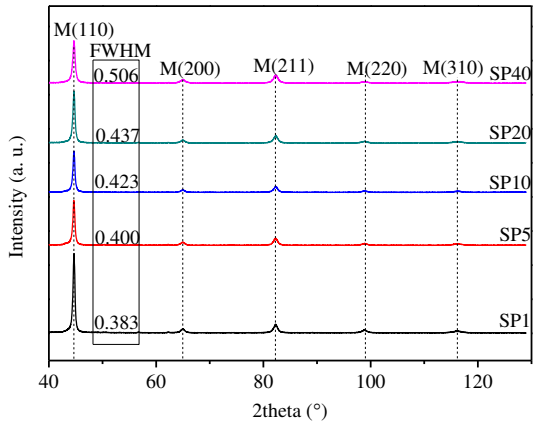

Fig. 7 XRD analysis of peened gears. SP1 (100%),

SP5 (500%), SP10 (1000%), SP20 (2000%), SP40 (4000%).

3.3.2 Microstrain and dislocation density estimation

According to Eq. 1 and Eq. 2, the relation scatter diagram between $\delta \cdot \cos\theta/\lambda$ and $2 \cdot \sin\theta/\lambda$ for different diffraction peaks is shown in Fig. 8. The slope which represents strain ε is obtained by linear fitting, and dislocation density can be calculated using Eq. 3. Fig. 9 shows the variations of microstrain and dislocation density with coverage near the tooth surface. It is revealed from results that microstrain and dislocation density increase slowly with shot peening coverage levels. The microstrain ranges from 0.008 to 0.0126, whereas the dislocation density ranges from 1.52×10^{16} m^{-2} to 3.70×10^{16} m^{-2}. Dislocation density is related to microstrain, so it is shown that the calculated dislocation density has the same trend with the microstrain on the gear tooth flanks.

Shot peening induces cyclic plastic deformation on the gear tooth flank, and the process of plastic deformation is in fact the result of dislocation movement on the surface layer. Greater deformation resistance results in a stronger ability to hinder the dislocation movement. Compressive residual stress induced by the shot peening offsets the external load, which indicates that shot peening reduces the driving force for the dislocation movement and hinders the crystal slip on the surface layer. The dislocation density increases due to the increase of strain after shot peening; with the increase of coverage, dislocation tangle, interaction, and pile-up take place in the material and then evolve into subgrain boundaries in this process; finally the grains are refined [54,55]. This phenomenon is becoming more and more serious as coverage increases. It is logical that grain refinement represents the increase of grain boundary, which provides better resistance to the dislocation movement for the material. Consequently, the hardness of the material can be enhanced at the macroscopic level.

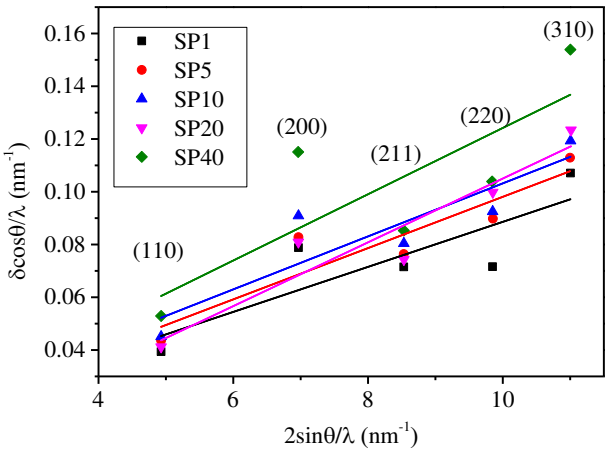

Fig. 8 Williamson-Hall plots for peened gears. SP1 (100%), SP5 (500%), SP10 (1000%), SP20 (2000%), SP40 (4000%).

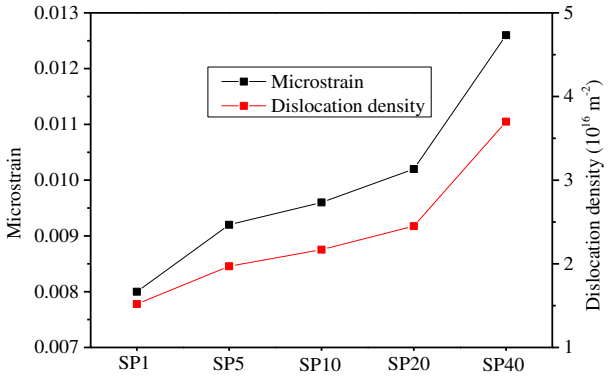

Fig. 9 Microstrain and dislocation density of gears. SP1 (100%), SP5 (500%), SP10 (1000%), SP20 (2000%), SP40 (4000%).

4 Conclusions

(1) Under the coverage of 100%~4000%, the top surface residual stress is in the range of −518.53 to −634.71 MPa, whereas the maximum residual stress varies from −852.63 to −1120 MPa. The maximum compressive residual stress for coverage levels less than 1000% exhibits obvious growth tendency with coverage. However, there are no significant variations in the magnitude of maximum compressive residual stress beyond the coverage of 1000%. There exists a saturation value for maximum residual compressive stress.

(2) Shot peening can enhance the surface hardness from 656.5 to 747.5 $HV_{1.0}$. Near-surface hardness on the tooth flank is positively correlated with coverage levels, but it has a saturation value. Beyond the coverage of 1000%, the increasing trend of the

hardness peak slows down.

(3) The roughness value on the gear tooth flank can be reduced if the coverage is appropriately increased. Beyond the coverage of 1000%, numerous damages are easily created on the gear surface in the form of microscalings, spallings, burrs, etc., which cause crack initiation.

(4) W-H method is used to calculate the microstrain and dislocation density on the tooth surface under different shot peening coverage levels. The dislocation density is in the order of 10^{16} m^{-2} under the coverage of 100%~4000%, whereas the microstrain ranges from 0.0085 to 0.0126.

(5) Taking into consideration of service lifetime, working noise and economic efficiency, the coverage of 1000% is the optimal coverage for heavy-duty-axle gears in shot peening.

Declarations section

a. Funding information

This work was supported by the National Natural Science Foundation of China (grant no. 52075552, 51805552, 51805555) and Innovation and Entrepreneurship Technology Investment Project of Hunan Province (grant no. 2019GK5032). Thanks to Mr. Zhou Jibo, Hande axle (Zhuzhou) Gear Co., Ltd. for the provision of shot peening treatment.

b. Conflicts of interest

The author declared that they have no conflicts of interest to this work. We declare that we do not have any commercial or associative interest that represents a conflict of interest in connection with the work submitted.

c. Availability of data and material

The author declared that our data and material are available.

d. Code availability

Not applicable.

e. Ethics approval

Not applicable.

f. Consent to participate

We confirm.

g. Consent for publication

We confirm.

h. Authors' contributions

Hongzhi Yan: Conceptualization; Funding acquisition; Formal analysis; Methodology; Investigation; Writing. Pengfei Zhu: Data curation; Investigation; Resources; Formal analysis; Writing. Zhi Chen: Funding acquisition; Investigation; Methodology; Validation. Hui Zhang: Data curation; Investigation. Yin Zhang: Data curation. Yu Zhang: Data curation; Funding acquisition.

References

1. Cao W, Ren S, Pu W, et al (2020) Microstress cycle and contact fatigue of spiral bevel gears by rolling-sliding of asperity contact. Friction 8:1083–1101
2. Zhang JG, Liu SJ, Fang T (2017) On the prediction of friction coefficient and wear in spiral bevel gears with mixed TEHL. Tribol Int 115:535–545
3. (2019) Shot peening applications. Metal Improvement Company, Paramus
4. Lawerenz M, Ekis I (1992) Creating an in-house shot peening specification for gears Part 1. Shot Peener 6:13–18
5. Haga S, Harada Y, Tsubakino H (2005) Relation between microstructure of shot-peening steel and its mechanical characteristics. In: Proceedings of the 9th international conference on shot peening, Paris, France, pp 460–465
6. Champaigne J (2001) Shot peening overview, Electronics Inc., Mishawaka
7. Mo S, Zhu SP, Jin JJ, et al (2018) Lubrication characteristics of gear after shot peening base on 25-pellet model. Adv Mech Eng 10:1687814018790655
8. Mo S, Zhang T, Jin GG, et al (2018) Elastohydrodynamic lubrication characteristics of spiral bevel gear subjected to shot peening treatment. Math Probl Eng 2018:3043712
9. Mo S, Feng ZY, Jin GG, et al (2019) Research on tribological characteristics of bevel gear after shot blasting based on 85-pellets model. P I Mech Eng J-J Eng 233:1074–1089
10. Santa-aho S, Sorsa A, Wartiainen J, et al (2018) Surface layer characterization of shot peened gear specimens. MPC 7:807–826

11. Matsui K, Eto H, Yukitake K, et al (2002) Increase in fatigue limit of gears by compound surface refining using vacuum carburizing, contour induction hardening and double shot peening. JSME Int J A-Solid M 45:290–297
12. Cammett J (2007) Shot peening coverage—the real deal. Shot Peener 21:8–14
13. Shahid L, Janabi-Sharifi F, Keenan P (2017) Image segmentation techniques for real-time coverage measurement in shot peening processes. Int J Adv Manuf Tech 91:859–867
14. AGMA (2017) AGMA standard 938-A05—shot peening of gears. AGMA
15. SAE (2013) SAE standard J2277—shot peeing coverage determination. Surface Enhancement Committee, SAE International
16. Sakamoto J, Lee YS, Cheong S K (2014) Effect of shot peening coverage on fatigue limit in round bar of annealed medium carbon steel. J Mech Sci Technol 28:3555–3560
17. Wu JZ, Liu HJ, Wei PT, et al (2020) Effect of shot peening coverage on hardness, residual stress and surface morphology of carburized rollers. Surf Coat Tech 384:125273
18. Maleki E, Unal O (2018) Roles of surface coverage increase and re-peening on properties of AISI 1045 carbon steel in conventional and severe shot peening processes. Surf Interfaces 11:82–90
19. Maleki E, Unal O, Kashyzadeh KR (2019) Efficiency analysis of shot peening parameters on variations of hardness, grain size and residual stress via taguchi approach. Met Mater Int 25:1436–1447
20. Inoue K, Maehara T, Yamanaka M, et al (1989) The effect of shot peening on the bending strength of carburized gear teeth. JSME Int J 32:448–454
21. Alsumait A, Li Y, Weaser M, et al (2019) A comparison of the fatigue life of shot-peened 4340m steel with 100, 200, and 300% coverage. J Mater Eng Perform. 28:1780–1789
22. Qiang B, Li YD, Yao CR, et al (2018) Effect of shot peening coverage on residual stress field and surface roughness. Surf Eng 34:939–946
23. SAE (2017) SAE standard J443—procedures for using standard shot peening test strip. Surface Enhancement Committee, SAE International
24. ASTM (2019) ASTM Standard E915-19—standard test method for verifying the alignment of X-ray diffraction instrumentation for residual stress measurement. ASTM International
25. British Standards Institution (2008) British Standard BS EN 15305—nondestructive testing—test method for residual stress analysis by X-ray diffraction. Standard Policy and Strategy Committee
26. Moore MG, Evans WP (1958) Mathematical correction for stress in removed layers in X-ray diffraction residual stress analysis. SAE Trans 66:340–345
27. Takebayashi S, Kunieda T, Yoshinaga N, et al (2010) Comparison of the dislocation density in martensitic steels evaluated by some X-ray diffraction methods. Isij Int 50:875–882
28. Williamson GK, Smallman RE (1956) III. Dislocation densities in some annealed and cold-worked metals from measurements on the X-ray debye-scherrer spectrum. Philos Mag 1:34–46
29. Pour-Ali S, Kiani-Rasshid AR, Babakhani A, et al (2018) Correlation between the surface coverage of severe shot peening and surface microstructural evolutions in AISI 321: A TEM, FE-SEM and GI-XRD study. Surf Coat Tech 334:461–470
30. Xiang SQ, Zhang XF (2019) Dislocation structure evolution under electroplastic effect. Mat Sci Eng A-Struct761:138026
31. Schiffner K, Helling CDG (1999) Simulation of residual stresses by shot peening. Comput Struct 72:329–340
32. González J, Peral LB, Colombo C, et al (2018) A study on the microstructural evolution of a low alloy steel by different shot peening treatments. Metals-Basel 8:187
33. Fathallah R, Sidhom H, Braham C, et al (2003) Effect of surface properties on high cycle fatigue behaviour of shot peened ductile steel. Mater Sci Technol 19:1050–1056
34. Nordin E, Alfredsson B (2017) Experimental

investigation of shot peening on case hardened SS2506 gear steel. Exp Techniques 41:433–451
35. Tagowski M, Czarnecki H (2016) Changes of surface layer properties in gear teeth after shot peening. Tribologia. 267:171–181
36. Ho HS, Li DL, Zhang EL, et al (2018) Shot peening effects on subsurface layer properties and fatigue performance of case-hardened 18CrNiMo7-6 steel. Adv Mater Sci Eng 2018:3795798
37. Lv Y, Lei LQ, Sun LN (2016) Influence of different combined severe shot peening and laser surface melting treatments on the fatigue performance of 20CrMnTi steel gear. Mat Sci Eng A-Struct 658:77–85
38. ISO (2012) Irish Standard I. S. EN ISO 25178-2—geometrical product specifications (GPS)—surface texture: areal—part 2: terms, definitions and surface texture parameters. NSAI
39. Unal O, Varol R (2014) Almen intensity effect on microstructure and mechanical properties of low carbon steel subjected to severe shot peening. Appl Surf Sci 290:40–47
40. Pour-Ali S, Kiani-Rashid AR, Babakhani A, et al (2018) Severe shot peening of AISI 321 with 1000% and 1300% coverages: A comparative study on the surface nanocrystallization, phase transformation, sub-surface microcracks, and microhardness. Int J Mater Res 109:451–459
41. Cammett J (2014) Are you peening too much. Shot Peener 28:10–14
42. Bagherifard S, Guagliano M (2012) Fatigue behavior of a low-alloy steel with nanostructured surface obtained by severe shot peening. Eng Fract Mech 81:56–68
43. Nam YS, Jeong YI, Shin BC, et al (2015) Enhancing surface layer properties of an aircraft aluminum alloy by shot peening using response surface methodology. Mater Design 83:566–576
44. Zhang YL, Lai FQ, Qu SG, et al (2020) Effect of shot peening on residual stress distribution and tribological behaviors of 17Cr2Ni2MoVNb steel. Surf Coat Tech 386:125497
45. Maleki E, Unal O, Amanov A (2018) Novel experimental methods for the determination of the boundaries between conventional, severe and over shot peening processes. Surf Interfaces 13:233–254
46. Hassani-Gangaraj SM, Moridi A, Guagliano M, et al (2014) The effect of nitriding, severe shot peening and their combination on the fatigue behavior and micro-structure of a low-alloy steel. Int J Fatigue 62:67–76
47. Liu HF, Wei YF, Tan CKI, et al (2020) XRD and EBSD studies of severe shot peening induced martensite transformation and grain refinements in austenitic stainless steel. Mater Charact 168:110574
48. Fu P, Zhan K, Jiang CH (2013) Micro-structure and surface layer properties of 18CrNiMo7-6 steel after multistep shot peening. Mater Design 51:309–314
49. Lv YH, Gai DY, Song YQ, et al (2015) Effect of carburizing and shot peening on the microstructure and surface properties of 17-CrNi6-Mo steel. Strength Mater 47:47–55
50. Fu P, Jiang CH (2014) Residual stress relaxation and micro-structural development of the surface layer of 18CrNiMo7-6 steel after shot peening during isothermal annealing. Mater Design 56:1034–1038
51. Saklakoglu N, Bolouri A, Irizalp SG, et al (2021) Effects of shot peening and artificial surface defects on fatigue properties of 50CrV4 steel. Int J Adv Manuf Tech 112:2961–2970
52. Maleki E, Farrahi GH, Kashyzadeh KR, et al (2020) Effects of conventional and severe shot peening on residual stress and fatigue strength of steel AISI 1060 and residual stress relaxation due to fatigue loading: experimental and numerical simulation. Met Mater Int
53. Ranaware PG, Rathod MJ (2017) Shot peening in a novel centrifugal air blast reactor. Surf Eng 33:667–678
54. Prakash NA, Gnanamoorthy R, Kamaraj M (2012) Surface nanocrystallization of aluminium alloy by controlled ball impact technique. Surf Coat Tech 210:78–89
55. Bagheri S, Guagliano M (2009) Review of shot peening processes to obtain nanocrystalline surfaces in metal alloys. Surf Eng 25:3–14

Figures

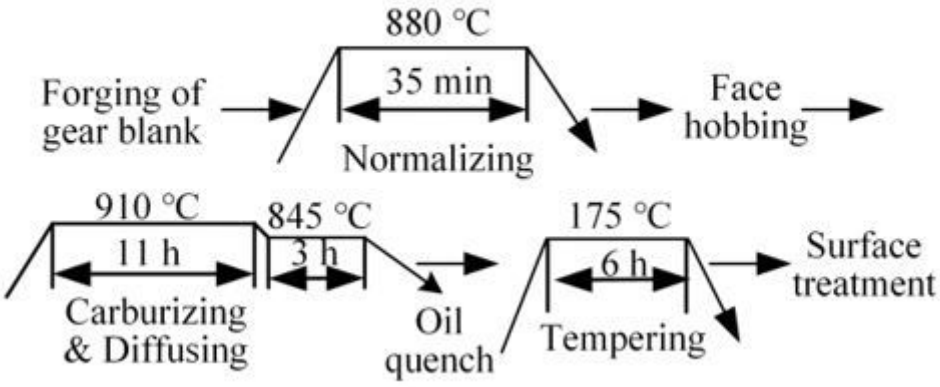

Figure 1

Machining and heat-treatment process

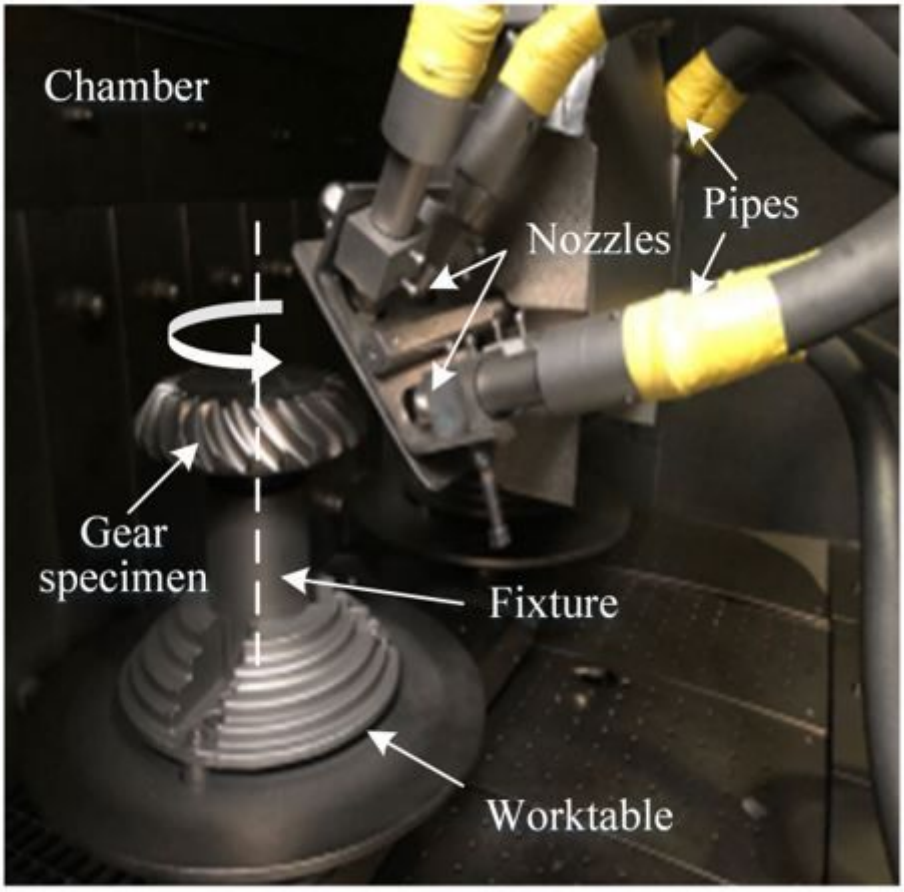

Figure 2

Shot peening of the gear

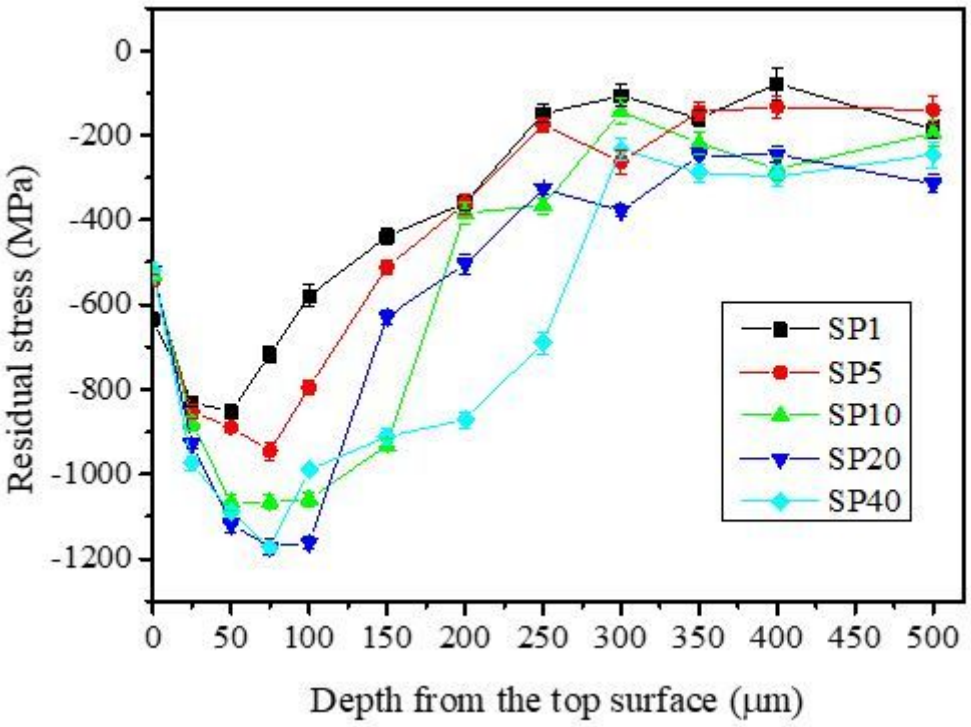

Figure 3

Residual stress depth profiles in the gear profile direction. SP1 (100%), SP5 (500%), SP10 (1000%), SP20 (2000%), SP40 (4000%).

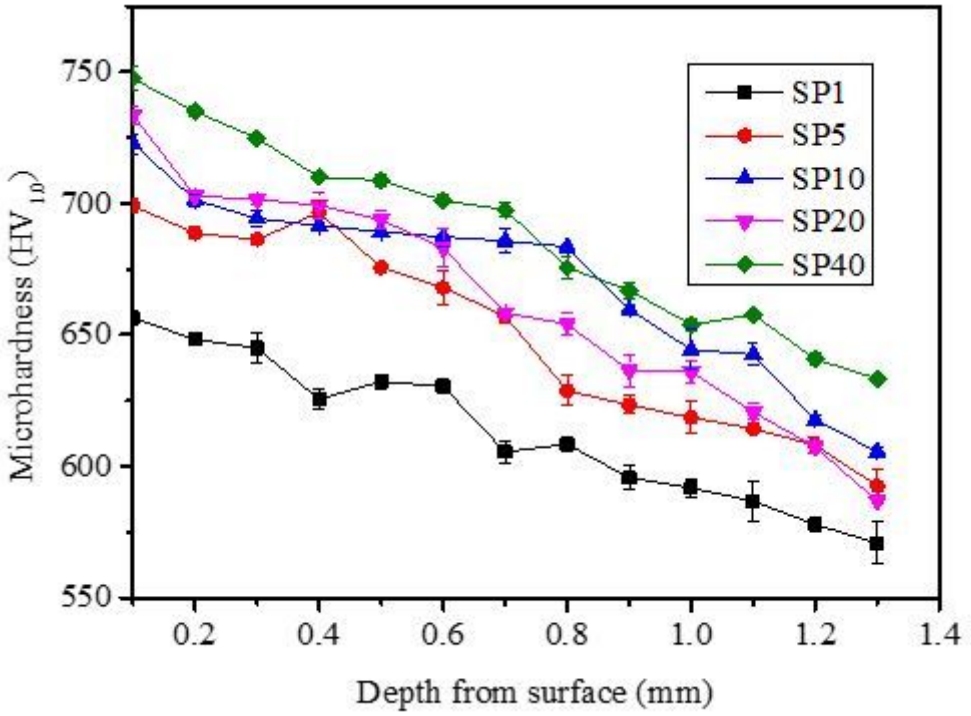

Figure 4

Microhardness distributions. SP1 (100%), SP5 (500%), SP10 (1000%), SP20 (2000%), SP40 (4000%).

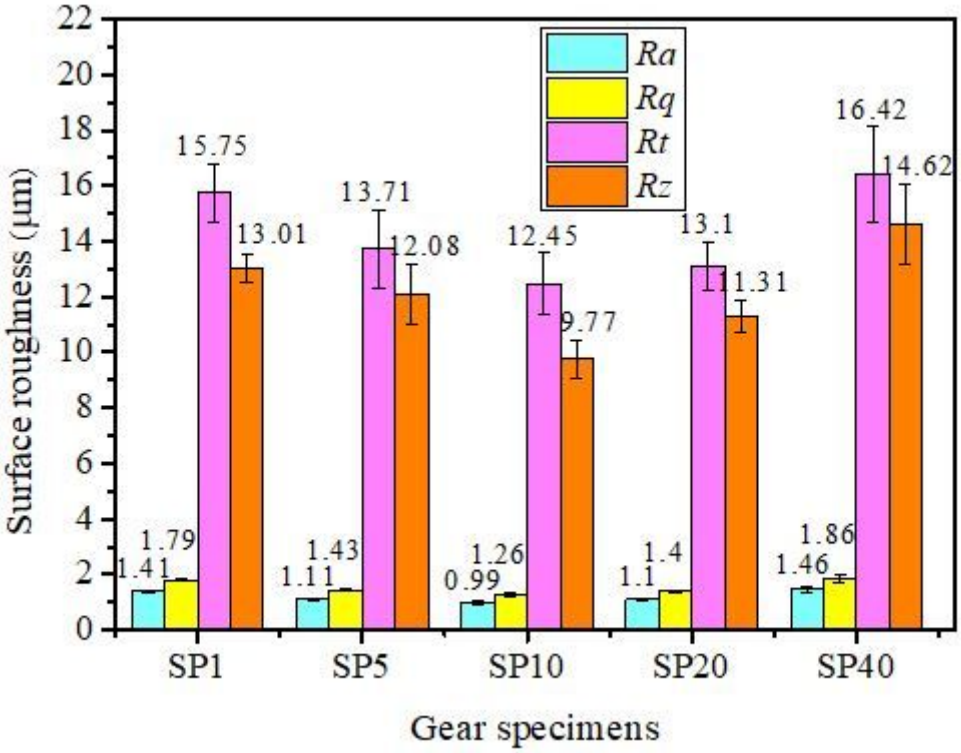

Figure 5

Surface roughness evolution. SP1 (100%), SP5 (500%), SP10 (1000%), SP20 (2000%), SP40 (4000%).

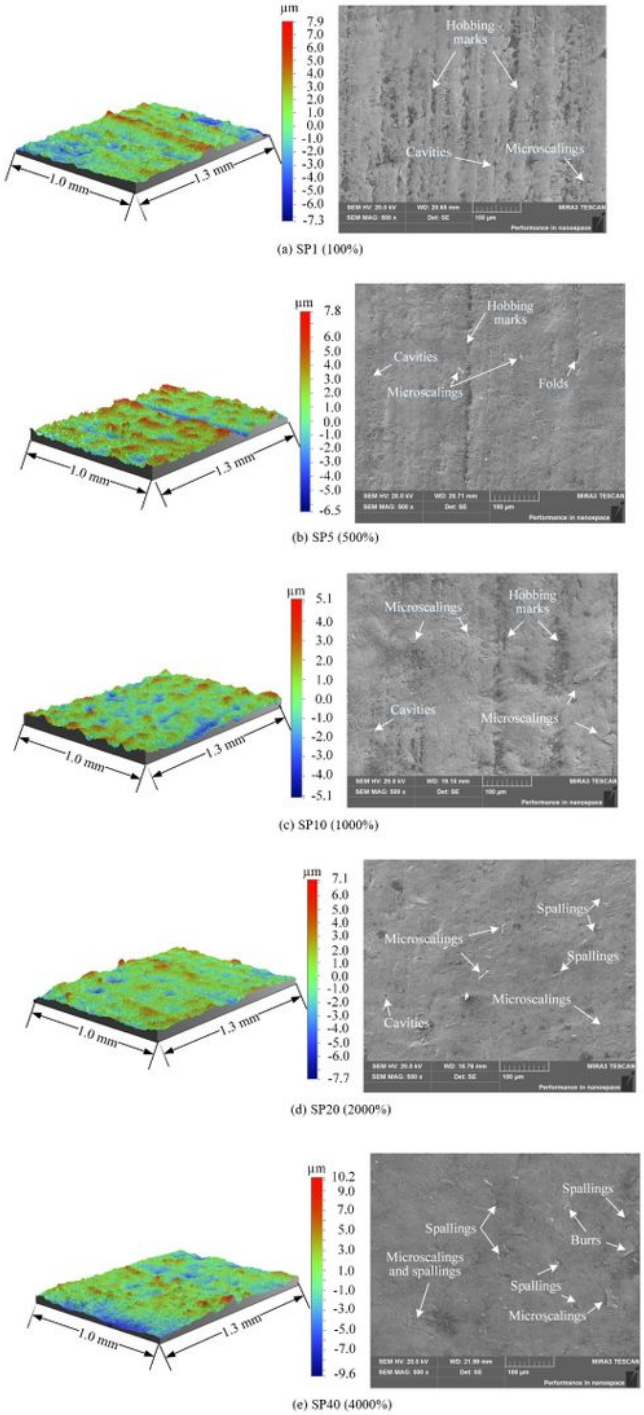

Figure 6

Surface roughness profiles (left) and SEM images (right)

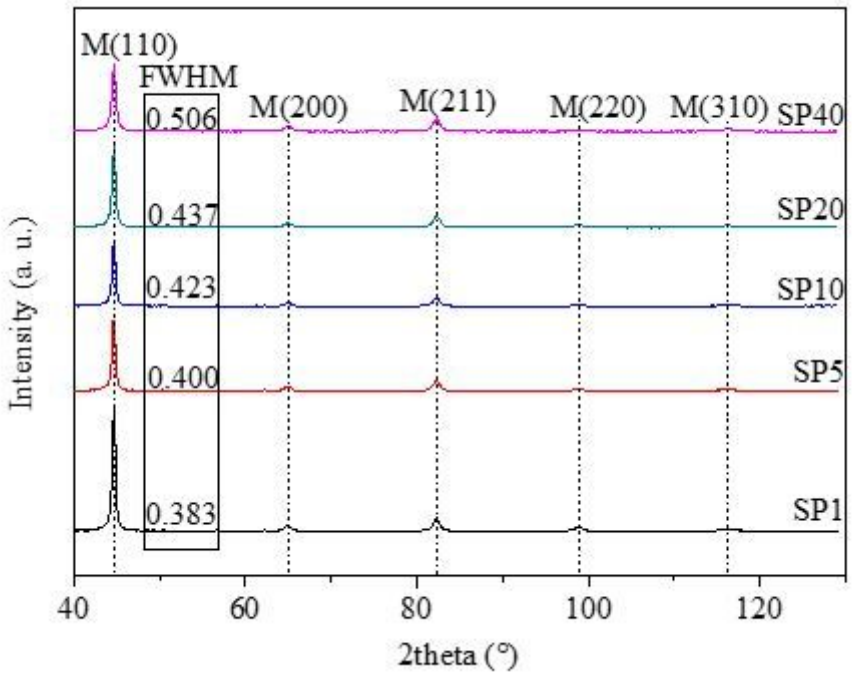

Figure 7

XRD analysis of peened gears. SP1 (100%), SP5 (500%), SP10 (1000%), SP20 (2000%), SP40 (4000%).

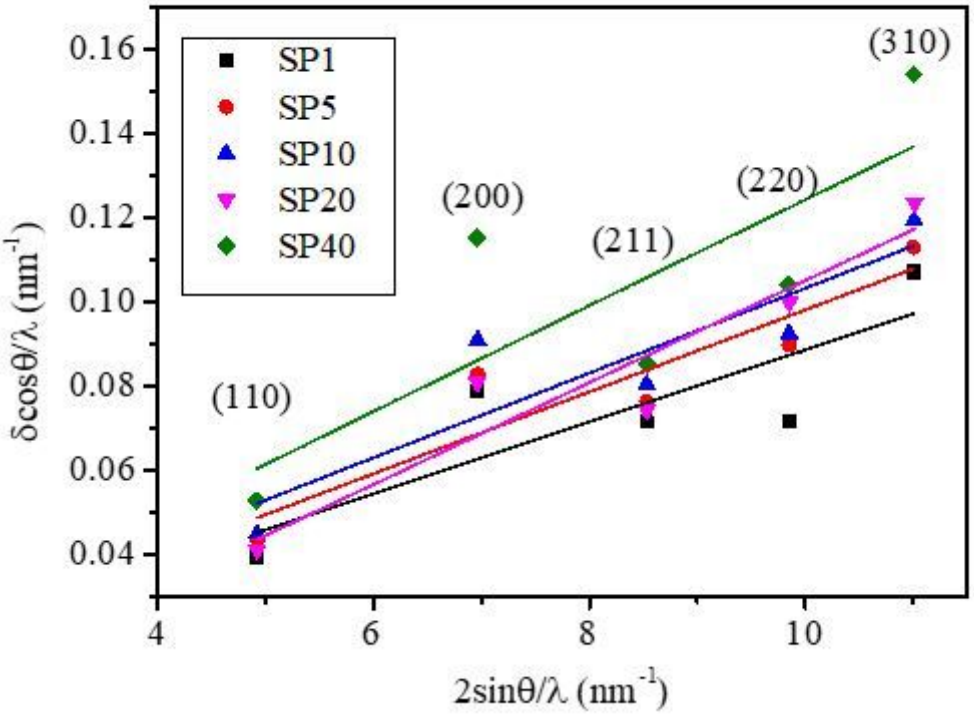

Figure 8

Williamson-Hall plots for peened gears. SP1 (100%), SP5 (500%), SP10 (1000%), SP20 (2000%), SP40 (4000%).

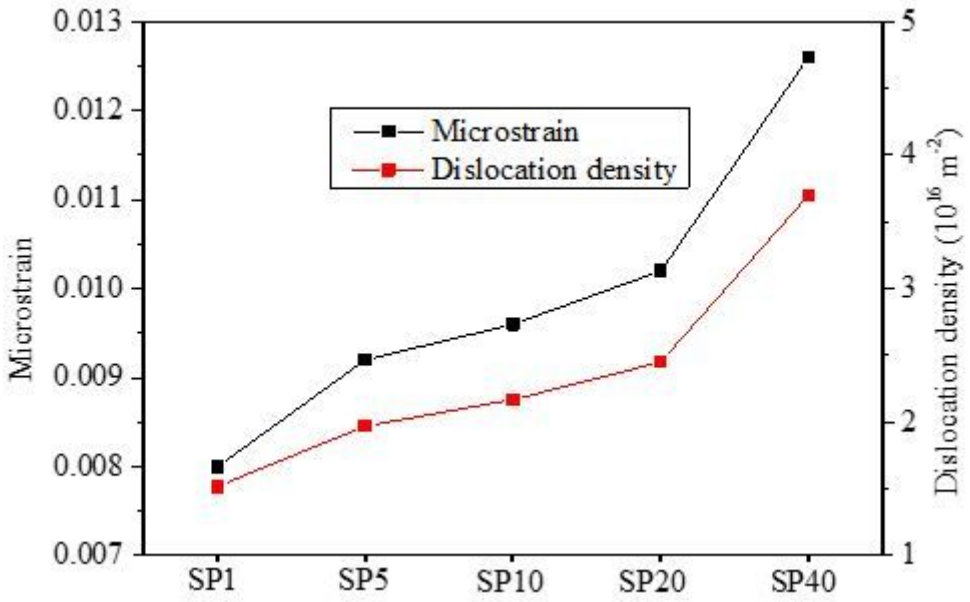

Figure 9

Microstrain and dislocation density of gears. SP1 (100%), SP5 (500%), SP10 (1000%), SP20 (2000%), SP40 (4000%).